Hindawi Publishing Corporation
Journal of Biomedicine and Biotechnology
Volume 2012, Article ID 178487, 9 pages
doi:10.1155/2012/178487

Research Article

Electric-Field-Directed Self-Assembly of Active Enzyme-Nanoparticle Structures

Alexander P. Hsiao[1] and Michael J. Heller[1,2]

[1] *Department of Bioengineering, University of California San Diego, La Jolla, CA 92093-0412, USA*
[2] *Department of NanoEngineering, University of California San Diego, La Jolla, CA 92093-0412, USA*

Correspondence should be addressed to Michael J. Heller, mheller@ucsd.edu

Received 2 September 2011; Accepted 13 October 2011

Academic Editor: Seunghun Hong

A method is presented for the electric-field-directed self-assembly of higher-order structures composed of alternating layers of biotin nanoparticles and streptavidin-/avidin-conjugated enzymes carried out on a microelectrode array device. Enzymes included in the study were glucose oxidase (GOx), horseradish peroxidase (HRP), and alkaline phosphatase (AP); all of which could be used to form a light-emitting microscale glucose sensor. Directed assembly included fabricating multilayer structures with 200 nm or 40 nm GOx-avidin-biotin nanoparticles, with AP-streptavidin-biotin nanoparticles, and with HRP-streptavidin-biotin nanoparticles. Multilayered structures were also fabricated with alternate layering of HRP-streptavidin-biotin nanoparticles and GOx-avidin-biotin nanoparticles. Results showed that enzymatic activity was retained after the assembly process, indicating that substrates could still diffuse into the structures and that the electric-field-based fabrication process itself did not cause any significant loss of enzyme activity. These methods provide a solution to overcome the cumbersome passive layer-by-layer assembly methods to efficiently fabricate higher-order active biological and chemical hybrid structures that can be useful for creating novel biosensors and drug delivery nanostructures, as well as for diagnostic applications.

1. Introduction

With recent advances in the assembly of nanoparticles (NPs) into higher-order structures and components, the ability to incorporate biologically active molecules has become more important [1, 2]. Considerable research efforts are now directed towards the fabrication and integration of biologically active molecules into NP structures that could be used in drug delivery, biological and chemical sensors, and diagnostics. In most cases, these higher-order structures are fabricated with passive layer-by-layer (LBL) techniques to self-assemble the molecules into organized structures through specific interactions including covalent binding, gold-thiol interactions, electrostatic interactions, and protein-ligand binding [3–11]. However, passive processes are concentration dependent and these methods require complex processes and long incubation times in high concentration solutions of molecules. Moreover, in order to direct the assembly onto specific sites, blocking agents or physical patterning such as lithography is necessary [12]. To circumvent these issues, active processes have been developed, including DC electrophoretic deposition and magnetic-field-assisted deposition [13–18]. Also, work has been carried out on the use of AC dielectrophoretic techniques to manipulate NPs [19–21]. The application of electric fields allows for rapid, site-directed concentration of macromolecules, polymers, and NPs to enhance the self-assembly process. Such methods have been employed to produce colloidal aggregates as well as pattern NPs atop electrode surfaces [17, 22–29]. In addition, nonspecific binding and high background, which play a crucial role in the incorporation and detection of biological molecules, can be reduced with electrode patterns which direct the molecules toward the active site where deposition is preferred and away from nonactive regions. More recently, the method of electrophoretic deposition has been applied to biological components. This powerful tool has enabled devices to be made which utilize the electric fields to enhance DNA

hybridization, to form protein layers for biosensors, and to pattern cells [30–36]. Recently we have shown the ability to construct higher-order NP structures by electric-field-directed self-assembly through the specific interactions of complementary DNA sequences as well as through protein-molecule interactions (Figures 1(a) and 1(b)) [14, 37, 38]. We now present the ability to integrate active enzymes into these NP structures by directed electrophoretic means (Figure 1(c)), thus providing a new bottom-up fabrication method for patterning and constructing structures from NPs in a rapid and combinatorial fashion atop a microarray.

2. Materials and Methods

2.1. CMOS Microarray Setup. An ACV 400 CMOS electronic microarray (Nanogen, Inc.), shown in Figure 2, which consists of 400 individually controllable 55 μm-diameter platinum electrodes was used for all layer assembly experiments. The microarray chip is overcoated by the manufacturer with a streptavidin-embedded polyacrylamide hydrogel which serves as a permeation layer. The device was computer controlled using ACV400 software. The software allowed each electrode to be configured to independently source 0 to 5 V or 0 to 1 μA per electrode, with each electrode on the array capable of being independently biased.

2.2. Chip Preparation. To prepare the chip surface as depicted in the cross-section in Figure 2, the microarray chip was first washed by pipetting 20 μL deionized water (dH_2O, Millipore, 18 MΩ) onto and off the chip a total of 10 times. Subsequently, 20 μL of a 2 μM biotin-dextran (Sigma) solution in dH_2O was pipetted onto the chip and allowed to incubate for 30 minutes at room temperature. The chip was then washed again with dH_2O, followed by incubation with 20 μL of a 1 mg/mL solution of streptavidin (Sigma) in dH_2O for 30 minutes at room temperature. Finally, the chip was washed with 100 mM L-histidine buffer and kept moist prior to use.

2.3. Preparation of NPs and Enzymes. Yellow-green fluorescent biotin-coated NPs, 200 nm and 40 nm in diameter (Molecular Probes, ex505, em515), were diluted to 0.01% (38 pM for 200 nm NPs and 4.7 nM for 40 nm NPs) in 100 mM L-histidine buffer. This suspension was vortexed and sonicated in a water bath for 15 minutes just prior to use to break up any aggregates. Additionally, glucose oxidase-avidin (GOx-avidin, Rockland) was diluted to 30 nM, streptavidin-alkaline phosphatase (streptavidin-AP, Sigma) was diluted to 40 nM, and streptavidin-peroxidase (streptavidin-HRP, Sigma) was diluted to 95 nM in 100 mM L-histidine buffer just prior to use.

2.4. DC Electric-Field-Directed Assembly of Streptavidin/Avidin Enzymes and Biotin NPs. NP and enzyme addressing conditions are derived from previous work [14]. In brief, 20 μL of the 200 nm biotin NP solution or enzyme solution was pipetted onto the chip. The selected electrodes were biased positive and activated with a constant DC current of 0.25 μA for 15 seconds to concentrate and assemble the particles or enzymes atop the activated electrodes. The solution was then removed and the chip washed with 20 μL of L-histidine buffer a total of three times. Assembly of the layer structures was achieved by alternating the addressing of biotin NPs with streptavidin/avidin enzymes. Every structure was capped with a final layer of biotin NPs. Different layer structures include layers of biotin NPs and GOx-avidin, layers of biotin NPs and streptavidin-AP, layers of biotin NPs and streptavidin-HRP, and layers of biotin NPs with alternate GOx-avidin and streptavidin-HRP to produce bienzyme structures. Identical conditions were employed to assemble layers of 40 nm biotin NPs with streptavidin-AP.

2.5. Monitoring of Layer Assembly by Fluorescence and ImageJ Calculations. Monitoring of layer growth was done by real-time imaging on an epifluorescent Leica microscope, with a Hamamatsu Orca-ER CCD using a custom LabVIEW interface. Images were acquired throughout the layering process and processed in ImageJ. For analysis, each image had its background subtracted with a rolling ball radius of 50. The image was then inverted and threshold fixed using the IsoData threshold. Manual adjustments were made to include as many electrodes as possible. A corresponding mask was generated to ensure each measured electrode area was identical. Raw integrated density values for each electrode were then acquired by mapping the data in the original image to the generated mask image.

2.6. Verification of Enzyme Activity via X-Ray Film. The verification of enzyme activity was performed on chips composed of alternate layers of 200 nm biotin NPs with either GOx-avidin or streptavidin-AP as the enzyme layers. All 400 electrodes on the array were activated to maximize the total number of fabrication sites for the layer structures. For the structures assembled with GOx-avidin, a reaction solution consisting of 227 mM glucose (Sigma), 8.4 mM luminol (Fluka), and 0.1 mg/mL peroxidase (Sigma) in 0.035 M Tris-HCl (pH 8.4) was prepared. The chips were washed with 100 mM L-histidine buffer and then with 0.1 M Tris-HCl (pH 8.0). Subsequently, 15 μL of the reaction solution was pipetted onto the chip surface. For chips with layer structures assembled using streptavidin-AP, the chips were washed with 100 mM L-histidine buffer and then 15 μL of CDP-star chemiluminescent reagent (Sigma) was dispensed onto the chips.

The chips were then wrapped in plastic wrap to prevent solution loss and placed into a cassette with X-ray film (Denville Scientific) for overnight exposure. The film was developed in a Hope MicroMax developer, scanned, and analyzed using ImageJ. The relative intensity from each chip was normalized to a chip that did not undergo layer assembly which was cleaned, prepared with the appropriate reaction solution, and exposed overnight as well.

2.7. Environmental Scanning Electron Microscopy (ESEM) of the Enzyme-NP Layers. After assembly of the enzyme-NP layers, the chip was washed multiple times with 100 mM

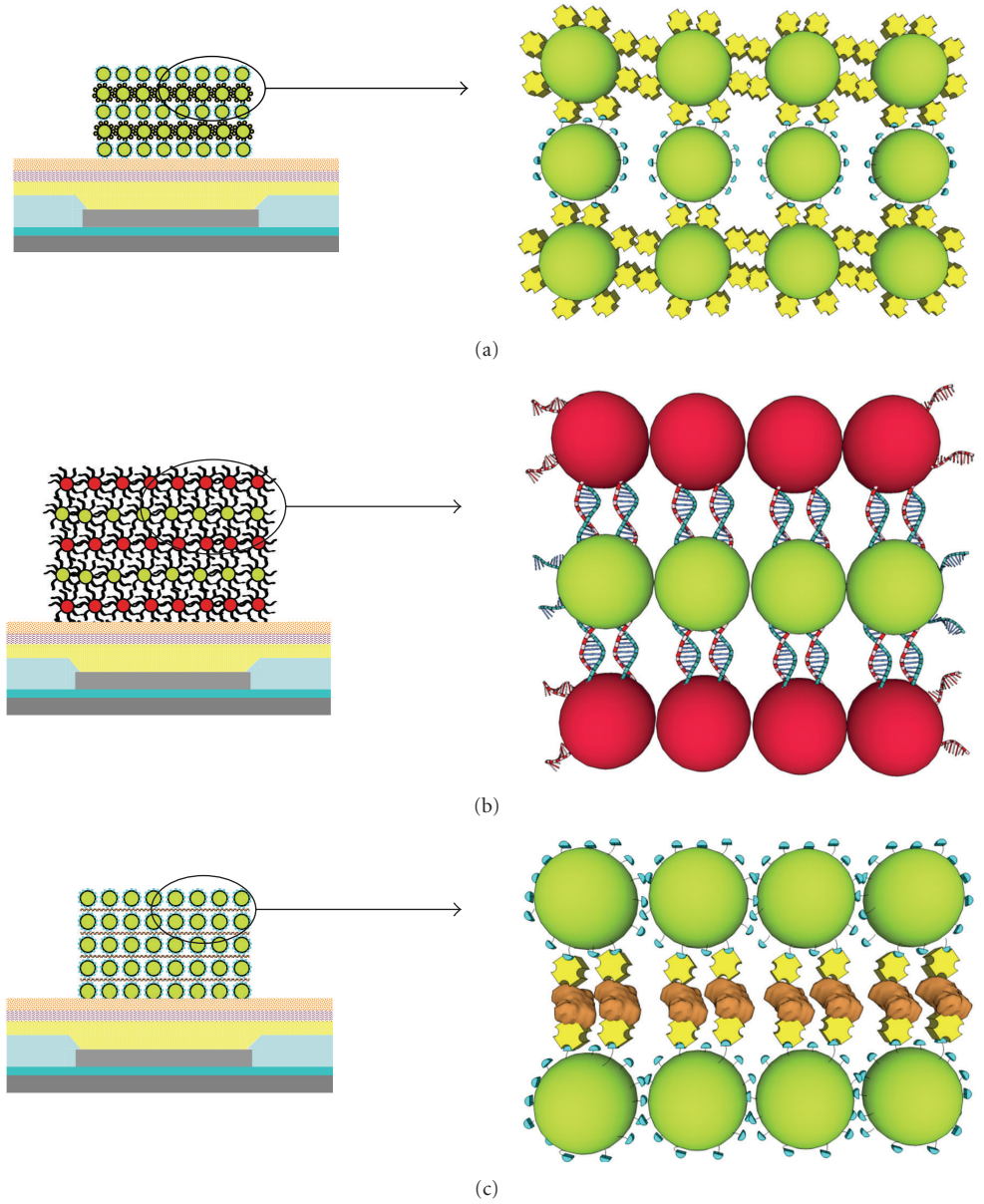

Figure 1: Electric-field-directed assembly (layering) of biomolecule NPs by different binding mechanisms: (a) NP layering with alternate biotin (blue)-functionalized NPs and streptavidin (yellow)-functionalized NPs. (b) NP layering by hybridization of complementary DNA sequences. (c) NP layering of biotin-functionalized NPs with streptavidin-functionalized enzymes (brown) (image not to scale).

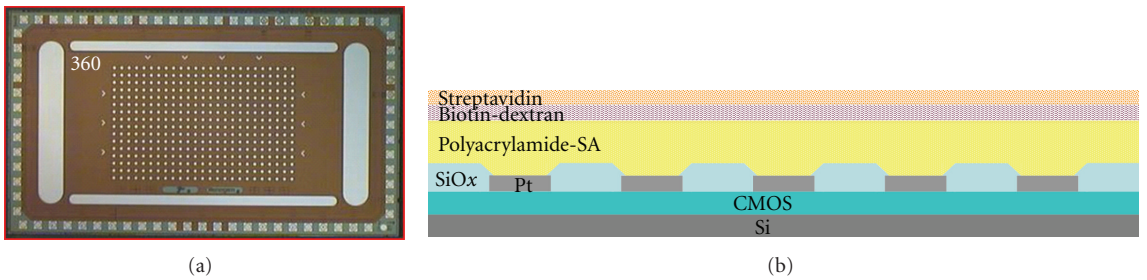

Figure 2: Images of the 400 site platinum electrode CMOS microelectronic array and a cross-section of the structure. The microarray is 4 mm × 7 mm, and each microelectrode is 55 μm in diameter.

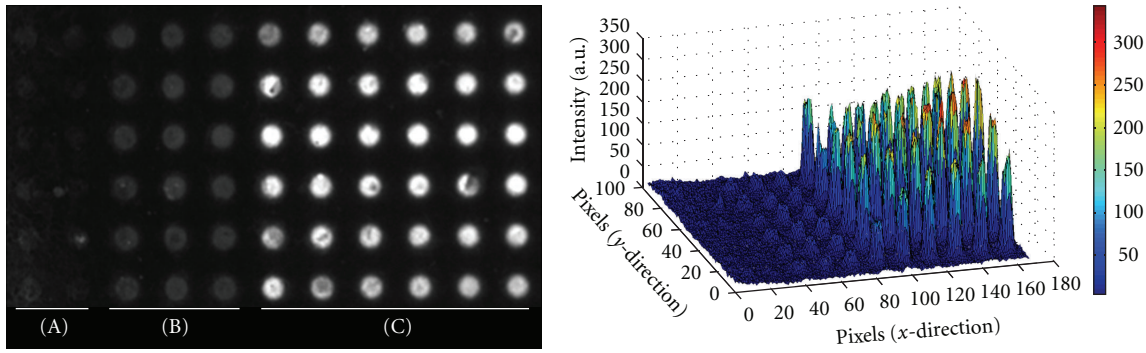

(a) (b)

Figure 3: (a) Fluorescence image of a section of the CMOS microarray after addressing 39 combined layers of biotin NPs and GOx-avidin. (A) No current applied. (B) Current applied ONLY when biotin NPs were addressed. (C) Current applied when BOTH biotin NPs and GOx-avidin were addressed. (b) Corresponding MATLAB plot of the relative fluorescence intensity (z-axis) of each electrode.

L-histidine buffer and then all solution was removed from the surface to allow the chip to dry. Chips were then coated with either 40 nm of gold sputtered via a Denton Discovery 18 sputter system or 40 nm of chromium via Denton IV desktop sputter coater. Fractures were introduced into the structures by careful cutting with a razor blade. Images were then acquired on a Phillips XL30 ESEM using a 10 kV beam in high vacuum mode.

3. Results and Discussion

3.1. Assembly of Enzyme-NP Layers and Verification of Proper Layer Formation. The assembly of NP layers was monitored by epifluorescence imaging; however, because only the biotin NPs are fluorescent, it was first important to verify that the NP-enzyme layers were forming as proposed by alternate layering of enzymes and NPs, as opposed to formation due to nonspecific interactions of the biotin NPs to themselves. This was done by organizing the electrodes into three specific regions, as shown in Figure 3(a). Region A consisted of microelectrodes which were never activated. This section served as a negative control to measure the amount of passive binding to the chip surface that would occur simply due to the presence of NPs and enzyme during alternate addressing steps. Region B consisted of microelectrodes only activated when the biotin NPs were addressed. This region served to measure the amount of non-specific binding of the NPs to themselves. Additionally, it served to show the amount of passive assembly that could occur if no enzyme was actively addressed to these microelectrode sites. Finally, region C consisted of microelectrodes which were activated during all addressing steps of NPs and enzymes. Microelectrodes in this region were expected to have proper formation of enzyme-NP layers. The results in Figures 3(a) and 3(b) indicate that the microelectrodes in region A have a fluorescent signal near that of the background, which is the surface of the chip between the electrodes, thus indicating that a very low number of fluorescent biotin NPs passively bound to the streptavidin surface at these sites. Microelectrodes in region B, which were only activated when biotin NPs were addressed, have a low level fluorescent signal and the microelectrodes in region C, which were activated when both NPs and GOx-avidin were addressed, have a high level fluorescent intensity indicating that multiple layers of NPs formed in region C. Comparison of fluorescence intensities between the three regions suggests that in order to construct higher-order structures both NPs and enzymes must be addressed to the same site, as in region C. If only biotin NPs are addressed, as in region B, the NPs will not bind to one another and no higher-order structures are formed; therefore, there is only low fluorescence intensity from the first layer of biotin NPs assembled onto the streptavidin chip surface. These results were verified with all three enzyme types and with both 200 nm and 40 nm NPs.

To corroborate with the fluorescence data, Figure 4 shows environmental scanning electron microscopy (ESEM) images of three microelectrode sites; one each for region A, B, and C after addressing 31 total layers of 200 nm biotin NPs and streptavidin-AP as well as 21 layers of 40 nm biotin NPs and streptavidin-AP on separate microarray chips. The microelectrodes from region A show only a small number of passively attached biotin NPs. The electrodes from region B show nearly a complete monolayer of biotin NPs, despite being exposed to 16 total addressing steps of biotin NPs. This demonstrates that there is little non-specific binding of the biotin particles to themselves; so despite the electric field directing additional NPs onto the first layer of NPs, they do not stick and are removed during the wash steps. The electrode from region C shows a high number of NPs assembled atop each other. Thus, active directed concentration of both the streptavidin/avidin enzyme and biotin NPs is necessary to assemble the higher-order structures and the layer assembly process does indeed proceed as designed. Additionally, the lack of particles on region A's microelectrodes further verifies that electric-field-directed assembly is efficient and can overcome the diffusion-limited process of passive LBL assembly. Each assembly step only required 15 seconds with NP and enzyme concentrations

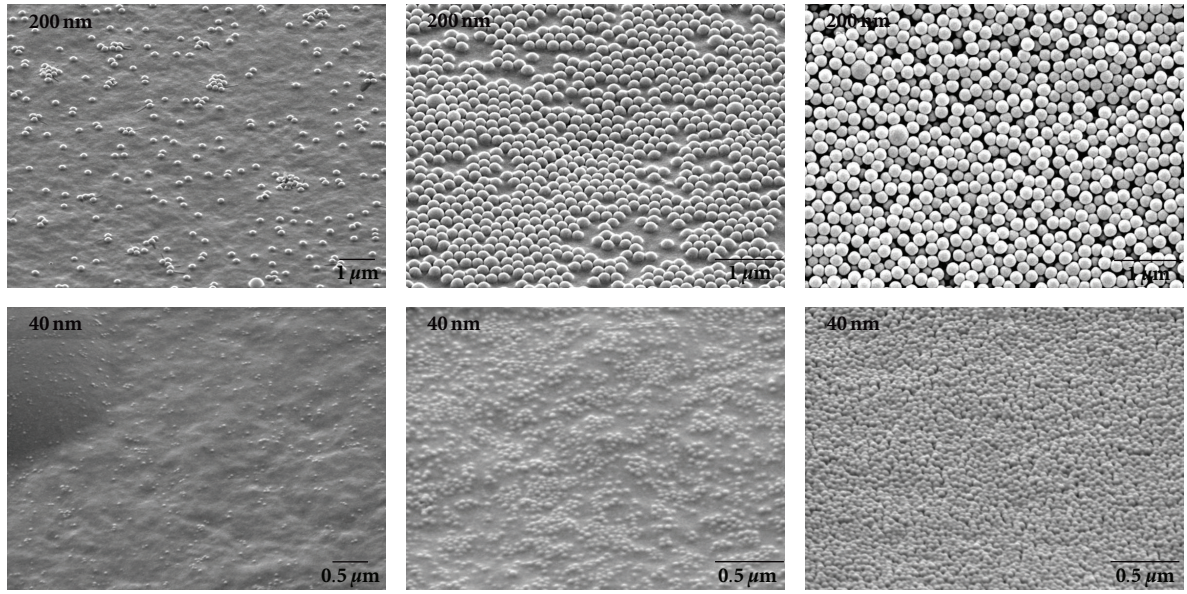

Figure 4: ESEM images of a microelectrode in each region (A), (B), and (C) after enzyme-NP assembly. Top row: microelectrodes after assembling 31 total alternating layers of 200 nm biotin NPs and streptavidin-AP. Bottom row: microelectrodes after assembling 21 layers of 40 nm biotin NPs and streptavidin-AP.

in the pM and nM range. At these time scales and NP and enzyme concentrations, no layers could be formed passively on the region A microelectrodes.

These results show that the electric field directed assembly technology is easily scalable to NPs of various sizes. This allows for tuning of the porosity of the final structures which may help control the (enzyme) substrate turnover and reaction kinetics, both of which would play crucial roles in biosensor devices. For drug delivery particles, the porosity will play a paramount role in the drug release profile. Moreover, we believe that integration of various types of NPs with different biomolecules would also be achievable as long as the proper binding elements are in place. Using multiple sized NPs would enable multiple porosities through the structure which may be needed to optimize reaction rates in multienzyme structures. Particles such as quantum dots could be incorporated to enhance detection. Moreover, using other biomolecules such as antibodies or DNA would allow the creation of a wide array of biosensors.

3.2. Monitoring NP Layer Assembly and Quality of Layers. Real-time layer assembly was monitored by visualizing increasing fluorescence intensity atop the microelectrode sites. Figure 5 shows a plot of the mean integrated density of fluorescence per microelectrode for microelectrodes in regions B and C of a microarray after 9, 19, 29, 39, and 47 total layers of 200 nm biotin NPs with alternate addressing of both GOx-avidin and streptavidin-HRP. From the plot, it is evident that the fluorescence for microelectrodes in region B, microelectrodes activated only when biotin NPs were addressed, maintains roughly the same fluorescence intensity throughout the layering experiments. These results further

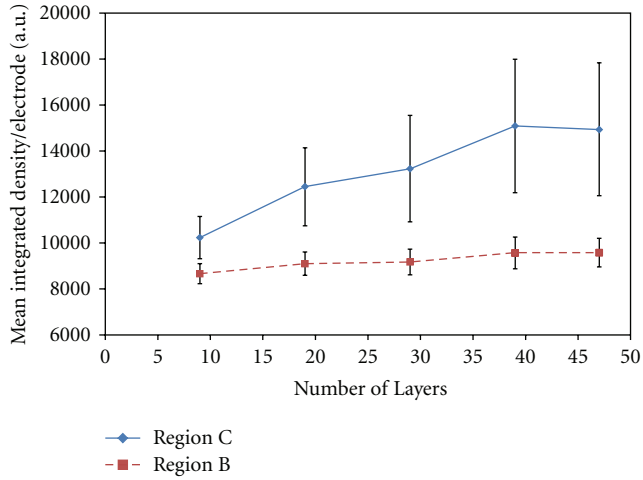

Figure 5: Plot showing the calculated mean integrated density per microelectrode for microelectrodes in regions B and C in bienzyme layer structures of 9, 19, 29, 39, and 47 total layers of 200 nm biotin NPs with alternate enzyme layer addressing of GOx-avidin and streptavidin-HRP.

substantiate the results in Figures 3 and 4 that without active electric-field-directed assembly of streptavidin/avidin-conjugated enzymes onto the biotin NPs there is no further layer assembly. Additionally, these results verify that multiple types of enzymes can be incorporated into the same structure as long as they are properly functionalized. In this case, there is a streptavidin-functionalized HRP and an avidin-functionalized GOx, both of which can bind to the biotin on the NPs and facilitate layer formation. The plot shows

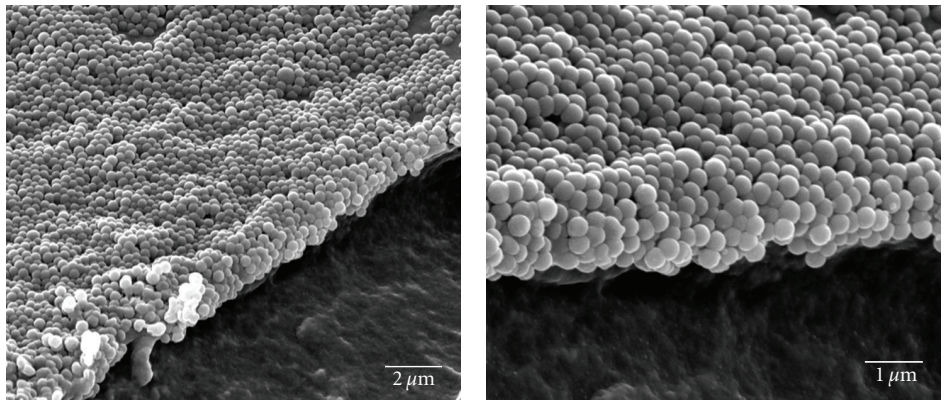

(a) (b)

Figure 6: ESEM images of 200 nm biotin NPs layered with GOx-avidin at introduced cuts showing the layering of NPs.

a trend of increasing mean fluorescence for microelectrodes in region C as the total number of layers increases. This is what is expected because as the number of layers increases there are more total fluorescent NPs on each microelectrode. The plot in Figure 5, however, does have quite a large amount of variability, which could be attributed to many factors. One factor could be the stoichiometry of the streptavidin conjugation to the enzyme. Streptavidin-HRP was conjugated at a 1 : 1 ratio and streptavidin-AP at a 2 : 1 ratio according to the manufacturer's specifications. Streptavidin-AP thus has 4 more available biotin binding sites per enzyme molecule. This increased availability of binding sites makes attachment to biotin NPs more robust and can lead to an increased quality of uniformity of NP layers. Thus, to enhance binding, enzymes can be conjugated with a higher ratio of streptavidin/avidin per enzyme. In addition, as the number of layers increases the stresses on the layer structure increase and the structure could shear or break apart more easily during washes. It is sometimes seen that atop a specific microelectrode the fluorescence intensity would suddenly decrease and this effect was believed to be due to layer fracture and particle loss. Again, a higher stoichiometry of streptavidin to protein would increase the binding interactions between layers and help to prevent structure fracture and NP loss. Finally, another factor could be attributed to nonuniformity in the electric field across the microarray chip or even across an individual microelectrode. This would also lead to variations in NP and enzyme assembly.

ESEM images, as seen in Figure 6, obtained at the edge of introduced fractures reveal the layering of the NPs atop the hydrogel layer. From these micrographs, it is evident that the assembled structures have variability in surface topography making it difficult to clearly distinguish one layer from the next. This is mostly attributed to the particle packing orientation as each additional layer of NPs packs onto the layer below. Additionally, this could be due to NP loss during the introduction of a fracture, during the sputtering of the metal overlayer for ESEM imaging, or even during the imaging process itself. In addition, there may be loss during washes and variations in binding across the electrode during the assembly process.

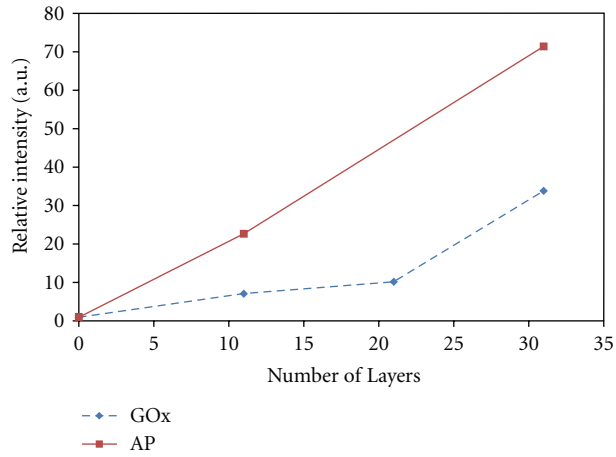

Figure 7: Plot of the relative intensity of chemiluminescent signal obtained from chips addressed with 0, 11, 21, and 31 layers of 200 nm biotin NPs and GOx-avidin or 0, 11, and 31 layers with streptavidin-AP.

3.3. Retention of Enzyme Activity. Retention of enzyme activity after layer assembly was evaluated by incubating the microarray chips with the appropriate chemiluminescent substrate and then exposing the chips to X-ray film. The results of the scanned and analyzed X-ray film detection of the enzyme-NP layers are shown in Figure 7. Data was collected from chips layered with 200 nm biotin NPs and GOx-avidin with 0, 11, 21, and 31 total layers as well as chips layered with 200 nm biotin NPs and streptavidin-AP at 0, 11, and 31 layers. The results show increasing activity detected with increasing numbers of layers. This trend is seen with both types of enzymes, and this indicates that the total enzyme activity can be tuned simply by altering the number of enzyme layers incorporated into each structure. Similar results could not be obtained from

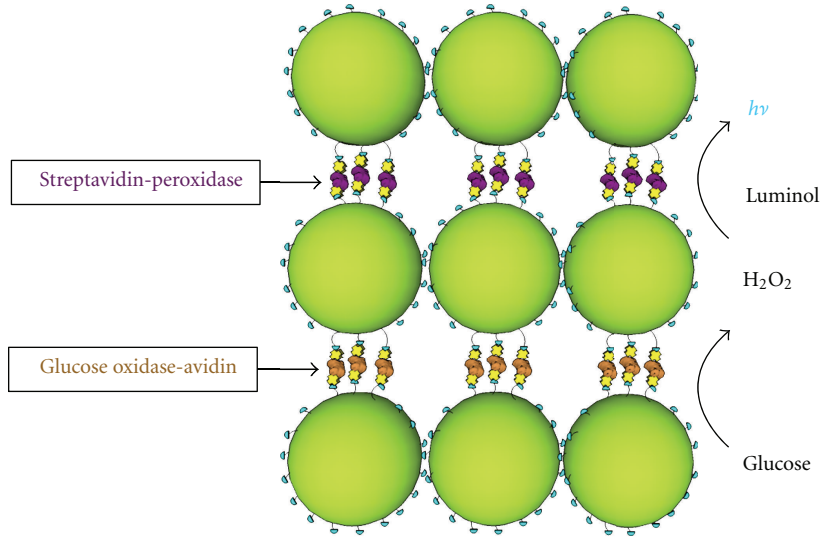

Figure 8: Coupling of bi-enzyme NP layers. The incorporation of both streptavidin-HRP and GOx-avidin into the same layer structure may allow for chemical coupling of the layers. The oxidation of glucose by GOx produces hydrogen peroxide which is then a substrate for the chemiluminescent oxidation of luminol, which generates light that can be detected.

bi-enzyme structures, consisting of both GOx-avidin and streptavidin-HRP, as illustrated in Figure 8. This may be due to a number of reasons including poor reagent and substrate quality, poor layer quality, poor structure porosity, insufficient enzyme incorporation into the layers, and a poor detection scheme. A bi-enzyme structure requires optimization due to the coupling of multiple reaction steps. If any one of the reactions is inefficient, then the overall signal may not be detectable. In addition, the products from the first reaction must be able to effectively diffuse to the second set of enzymes; thus, the enzyme layering order may be of importance. Additionally, an important aspect of producing active NP layers is the ability to sensitively detect their activity. The X-ray film used in the detection method verified in proof of principle that the biological activity of the molecules could be retained after assembly. More sensitive methods, including amperometric detection or highly sensitive imaging, beyond the capabilities of the microelectronic array and imaging system we had available, would allow for a better detection scheme to monitor total activity for each fabricated structure. Nonetheless, the presence of a measurable enzyme activity from the single enzyme structures verifies that the application of an electric field is not only efficient for structure assembly but also gentle enough to preserve the functionality of the enzymes.

Altogether the results showing enzyme-nanoparticle layer assembly and enzyme activity retention demonstrate an efficient and effective method of fabricating biological or chemical sensors. Site-specific layer assembly, demonstrated in this study as well as previous studies, means that multiple types of enzyme-nanoparticle structures can be fabricated on each chip in a combinatorial manner [37]. Additionally, various types of enzymes, proteins, or other biomolecules could be used in conjunction with a wide array of particle types as long as they have complementary binding mechanisms, such as the biotin-streptavidin scheme used here. This would allow for production of high-density microarray sensors capable of analyzing hundreds of analytes at a time.

4. Conclusion

We have successfully demonstrated the ability to fabricate higher-order enzyme-NP structures by electric-field-directed self-assembly. Through the application of electric-field-directed assembly, alternating layers of 200 nm or 40 nm biotin NPs and streptavidin/avidin enzymes have been assembled up to 47 layers. These structures included multilayer structures with 200 nm or 40 nm GOx-avidin-biotin NPs, with AP-streptavidin-biotin NPs, and with HRP-streptavidin-biotin NPs. The electrophoretic assembly method atop a microelectronic array allows for site-specific fabrication from low concentration solutions of enzymes and NPs. The concentration effect due to the electrophoretic deposition results in rapid layer assembly with minimal passive non-specific binding on inactive sites across the chip. Moreover, the enzymatic activity of the biological molecules was preserved in the assembled structures. In addition, we have assembled structures consisting of multiple enzyme types, GOx-avidin and streptavidin-HRP, which demonstrates the potential of multilevel reactions or detection schemes, including chemiluminescence and bioluminescence. This method of fabrication now provides an efficient mechanism of creating biologically and chemically active NP structures from individual components much more efficiently than traditional passive layer-by-layer methods. Assembly of these structures in a combinatorial manner to specific sites on the chip, using a wide array of biomolecules (proteins and DNA) and nanoparticles, would allow for

fabrication of high-density microarray sensors for high-throughput analysis. The ability to incorporate multiple types of molecules along with the potential of liftoff, which enables the detachment of these structures from the surface, renders them more versatile as dispersible biosensors, diagnostic tools, and drug delivery vehicles.

Acknowledgments

The authors thank Nanogen, Inc. for supplying microelectronic arrays and the Nanochip 400 system, Dr. Dietrich Dehlinger for assistance and training with the system and methods, Juhi Saha for her help in experiments, and the UCSD Nano3 facility and personnel for training and support on the ESEM.

References

[1] S. Guo and S. Dong, "Biomolecule-nanoparticle hybrids for electrochemical biosensors," *TrAC—Trends in Analytical Chemistry*, vol. 28, no. 1, pp. 96–109, 2009.

[2] K. Ariga, Q. Ji, and J. Hill, "Enzyme-encapsulated layer-by-layer assemblies: current status and challenges toward ultimate nanodevices," in *Advances in Polymer Science*, F. Caruso, Ed., vol. 229, pp. 51–87, Springer, Berlin, Germany, 2010.

[3] N. K. Chaki and K. Vijayamohanan, "Self-assembled monolayers as a tunable platform for biosensor applications," *Biosensors and Bioelectronics*, vol. 17, no. 1-2, pp. 1–12, 2002.

[4] Y. Kobayashi and J. I. Anzai, "Preparation and optimization of bienzyme multilayer films using lectin and glyco-enzymes for biosensor applications," *Journal of Electroanalytical Chemistry*, vol. 507, no. 1-2, pp. 250–255, 2001.

[5] B. Limoges, J. M. Savéant, and D. Yazidi, "Avidin-biotin assembling of horseradish peroxidase multi-monomolecular layers on electrodes," *Australian Journal of Chemistry*, vol. 59, no. 4, pp. 257–259, 2006.

[6] Y. Lvov, K. Ariga, I. Ichinose, and T. Kunitake, "Assembly of multicomponent protein films by means of electrostatic layer-by-layer adsorption," *Journal of the American Chemical Society*, vol. 117, no. 22, pp. 6117–6123, 1995.

[7] M. Onda, K. Ariga, and T. Kunitake, "Activity and stability of glucose oxidase in molecular films assembled alternately with polyions," *Journal of Bioscience and Bioengineering*, vol. 87, no. 1, pp. 69–75, 1999.

[8] M. Onda, Y. Lvov, K. Ariga, and T. Kunitake, "Sequential actions of glucose oxidase and peroxidase in molecular films assembled by layer-by-layer alternate adsorption," *Biotechnology and Bioengineering*, vol. 51, no. 2, pp. 163–167, 1996.

[9] K. L. Prime and G. M. Whitesides, "Self-assembled organic monolayers: Model systems for studying adsorption of proteins at surfaces," *Science*, vol. 252, no. 5010, pp. 1164–1167, 1991.

[10] S. V. Rao, K. W. Anderson, and L. G. Bachas, "Controlled layer-by-layer immobilization of horseradish peroxidase," *Biotechnology and Bioengineering*, vol. 65, no. 4, pp. 389–396, 1999.

[11] T. Hoshi, N. Sagae, K. Daikuhara, K. Takahara, and J. I. Anzai, "Multilayer membranes via layer-by-layer deposition of glucose oxidase and Au nanoparticles on a Pt electrode for glucose sensing," *Materials Science and Engineering C*, vol. 27, no. 4, pp. 890–894, 2007.

[12] X. M. Zhao, "Soft lithographic methods for nano-fabrication," *Journal of Materials Chemistry*, vol. 7, no. 7, pp. 1069–1074, 1997.

[13] S. Bharathi and M. Nogami, "A glucose biosensor based on electrodeposited biocomposites of gold nanoparticles and glucose oxidase enzyme," *Analyst*, vol. 126, no. 11, pp. 1919–1922, 2001.

[14] D. A. Dehlinger, B. D. Sullivan, S. Esener, and M. J. Heller, "Electric-field-directed assembly of biomolecular-derivatized nanoparticles into higher-order structures," *Small*, vol. 3, no. 7, pp. 1237–1244, 2007.

[15] S. Dey, K. Mohanta, and A. J. Pal, "Magnetic-field-assisted layer-by-layer electrostatic assembly of ferromagnetic nanoparticles," *Langmuir*, vol. 26, no. 12, pp. 9627–9631, 2010.

[16] M. Shao, X. Xu, J. Han et al., "Magnetic-field-assisted assembly of layered double hydroxide/metal porphyrin ultrathin films and their application for glucose sensors," *Langmuir*, vol. 27, no. 13, pp. 8233–8240, 2011.

[17] M. Trau, D. A. Seville, and I. A. Aksay, "Field-induced layering of colloidal crystals," *Science*, vol. 272, no. 5262, pp. 706–709, 1996.

[18] K. D. Barbee, A. P. Hsiao, M. J. Heller, and X. Huang, "Electric field directed assembly of high-density microbead arrays," *Lab on a Chip*, vol. 9, no. 22, pp. 3268–3274, 2009.

[19] R. Krishnan, D. A. Dehlinger, G. J. Gemmen, R. L. Mifflin, S. C. Esener, and M. J. Heller, "Interaction of nanoparticles at the DEP microelectrode interface under high conductance conditions," *Electrochemistry Communications*, vol. 11, no. 8, pp. 1661–1666, 2009.

[20] R. Krishnan and M. J. Heller, "An AC electrokinetic method for enhanced detection of DNA nanoparticles," *Journal of Biophotonics*, vol. 2, no. 4, pp. 253–261, 2009.

[21] R. Krishnan, B. D. Sullivan, R. L. Mifflin, S. C. Esener, and M. J. Heller, "Alternating current electrokinetic separation and detection of DNA nanoparticles in high-conductance solutions," *Electrophoresis*, vol. 29, no. 9, pp. 1765–1774, 2008.

[22] R. C. Bailey, K. J. Stevenson, and J. T. Hupp, "Assembly of micropatterned colloidal gold thin films via microtransfer molding and electrophoretic deposition," *Advanced Materials*, vol. 12, no. 24, pp. 1930–1934, 2000.

[23] L. Besra and M. Liu, "A review on fundamentals and applications of electrophoretic deposition (EPD)," *Progress in Materials Science*, vol. 52, no. 1, pp. 1–61, 2007.

[24] T. Haruyama and M. Aizawa, "Electron transfer between an electrochemically deposited glucose oxidase/Cu[II] complex and an electrode," *Biosensors and Bioelectronics*, vol. 13, no. 9, pp. 1015–1022, 1998.

[25] A. L. Rogach, N. A. Kotov, D. S. Koktysh, J. W. Ostrander, and G. A. Ragoisha, "Electrophoretic deposition of latex-based 3D colloidal photonic crystals: a technique for rapid production of high-quality opals," *Chemistry of Materials*, vol. 12, no. 9, pp. 2721–2726, 2000.

[26] L. Shi, Y. Lu, J. Sun et al., "Site-selective lateral multilayer assembly of bienzyme with polyelectrolyte on ITO electrode based on electric field-induced directly layer-by-layer deposition," *Biomacromolecules*, vol. 4, no. 5, pp. 1161–1167, 2003.

[27] Y. Solomentsev, M. Böhmer, and J. L. Anderson, "Particle clustering and pattern formation during electrophoretic deposition: a hydrodynamic model," *Langmuir*, vol. 13, no. 23, pp. 6058–6061, 1997.

[28] M. Trau, D. A. Saville, and I. A. Aksay, "Assembly of colloidal crystals at electrode interfaces," *Langmuir*, vol. 13, no. 24, pp. 6375–6381, 1997.

[29] S. R. Yeh, M. Seul, and B. I. Shraiman, "Assembly of ordered colloidal aggregates by electric-field-induced fluid flow," *Nature*, vol. 386, no. 6620, pp. 57–59, 1997.

[30] D. R. Albrecht, V. L. Tsang, R. L. Sah, and S. N. Bhatia, "Photo- and electropatterning of hydrogel-encapsulated living cell arrays," *Lab on a Chip*, vol. 5, no. 1, pp. 111–118, 2005.

[31] J. Cheng, E. L. Sheldon, A. Uribe et al., "Preparation and hybridization analysis of DNA/RNA from E. coli on microfabricated bioelectronic chips," *Nature Biotechnology*, vol. 16, no. 6, pp. 541–546, 1998.

[32] C. F. Edman, D. E. Raymond, D. J. Wu et al., "Electric field directed nucleic acid hybridization on microchips," *Nucleic Acids Research*, vol. 25, no. 24, pp. 4907–4914, 1997.

[33] C. Gurtner, E. Tu, N. Jamshidi et al., "Microelectronic array devices and techniques for electric field enhanced DNA hybridization in low-conductance buffers," *Electrophoresis*, vol. 23, no. 10, pp. 1543–1550, 2002.

[34] A. Kueng, C. Kranz, and B. Mizaikoff, "Amperometric ATP biosensor based on polymer entrapped enzymes," *Biosensors and Bioelectronics*, vol. 19, no. 10, pp. 1301–1307, 2004.

[35] R. G. Sosnowski, E. Tu, W. F. Butler, J. P. O'Connell, and M. J. Heller, "Rapid determination of single base mismatch mutations in DNA hybrids by direct electric field control," *Proceedings of the National Academy of Sciences of the United States of America*, vol. 94, no. 4, pp. 1119–1123, 1997.

[36] M. J. Heller, D. A. Dehlinger, and B. D. Sullivan, "Parallel assisted assembly of multilayer DNA and protein nanoparticle structures using a CMOS electronic array," in *International Symposium on DNA-Based Nanoscale Integration*, vol. 859 of *AIP Conference Proceedings*, pp. 73–81, May 2006.

[37] D. Dehlinger, B. Sullivan, S. Esener, D. Hodko, P. Swanson, and M. J. Heller, "Automated combinatorial process for nanofabrication of structures using bioderivatized nanoparticles," *Journal of the Association for Laboratory Automation*, vol. 12, no. 5, pp. 267–276, 2007.

[38] D. A. Dehlinger, B. D. Sullivan, S. Esener, and M. J. Heller, "Directed hybridization of DNA derivatized nanoparticles into higher order structures," *Nano Letters*, vol. 8, no. 11, pp. 4053–4060, 2008.